Excitation transfers within the fine structure of the $3\,^3D$ helium level in a helium glow discharge

A. Catherinot and B. Dubreuil
Groupe de Recherches sur l'Energétique des Milieux Ionisés Université d'Orléans, 45045 Orleans Cedex, France

G. Gousset
Centre de Recherche sur la Physique des Hautes Températures, Centre National de la Recherche Scientifique, Avenue de la Recherche Scientifique, 45045 Orleans Cedex, France

(Received 24 September 1979)

Fine-structure-changing collisions within the $3\,^3D$ state of atomic helium are investigated by a laser perturbation method in a helium low-pressure glow discharge. Measurements, performed for different experimental situations, lead to the determination of thermally averaged values for the excitation transfer cross sections: $\bar{\sigma}_{3\,^3D(J=1)\to 3\,^3D(J=2,3)} = 180 \pm 60$ Å^2 and $\bar{\sigma}_{3\,^3D(J=2,3)\to 3\,^3D(J=1)} = 42 \pm 5$ Å^2.

I. INTRODUCTION

While fine-structure-changing collisions have been widely studied for alkaline-rare-gas collisions,[1] few works have been devoted to the case of binary encounter of rare-gas atoms. In helium, to our knowledge, the only recently reported study concerns the estimation by a laser saturated-absorption experiment of the excitation transfer cross section between the $2\,^3P_1$ and $2\,^3P_2$ sublevels by collisions with ground-state atoms in a helium glow discharge.[2] As reported in a previous work dealing with excitation transfers in the $n=3$ He I sublevels,[3] an unexpected nonlinear behavior of the $3\,^3D$ state quenching rate coefficient has been observed for pressure values lower than 2 torr. This result was tentatively explained as being due to fine-structure-changing collisions. This hypothesis is confirmed by the study presented in this paper.

II. EXPERIMENT

The experimental device has been described in detail in previous papers dealing with radiative and collisional processes in helium,[3] hydrogen,[4] argon,[5] and nitrogen[6] glow discharges. Let us just recall the essential features of the experiment.

The excited helium states are populated in a capillary glow discharge, with pressure range $0.1 < P_{He} < 1$ (torr) and current intensity $10 < i < 50$ mA. The other characteristics of the discharge are the same as in Ref. 3.

For various experimental conditions, corresponding values of the electronic density are measured by a microwave cavity perturbation method ($10^{10} < n_e < 10^{11}$ cm^{-3}) and of the electronic mean kinetic energy are calculated from glow discharge theory ($3 < E < 20$ eV).

The gas temperature is measured by a thermocouple in contact with the discharge tube: $T_g = 325 \pm 5$ K. A tunable dye laser excited by a nitrogen laser (energy/pulse < 10 μJ, pulse width 4 nsec, spectral width 0.15 Å at 5876 Å) is used to induce a population perturbation on a selected state by optical pumping. The discharge is longitudinally traversed by the laser beam, and the fluorescence emitted by a cross section of the positive column is observed in a perpendicular direction by means of a 2-m grating spectrometer (resolving power 200 000 in order 2) and a photomultiplier tube. The time dependence of the laser-induced fluorescence light intensity $\Delta I(t)$ is analyzed by a Princeton Applied Research boxcar averager PAR 162 (time resolution 5 nsec) connected to a Data General minicomputer (Nova 3).

III. MEASUREMENTS

Recently improved in a laser saturated-absorption spectroscopy experiment,[2] very accurate measurements have been achieved on the $\lambda = 5876$-Å He I spectral-line structure ($3\,^3D \to 2\,^3P$ radiative transition) using level-crossing methods and radio-frequency spectroscopy.[7,8] As schematically shown in Fig. 1, this fine structure is composed of a group of components distributed on a 3.6-GHz range, 30 GHz away from the isolated one. Since the Doppler width at 325 K is about 4 GHz, the main part of the fine structure is hidden. Then the $\lambda = 5876$-Å He I line emitted by the positive column of our glow discharge appears to be composed of only two spectral components. The one centered at $\lambda = 5875.97$ Å is composed of the $3\,^3D_1 \to 2\,^3P_0$ transition alone, and the other, centered at $\lambda = 5875.63$ Å, contains the contributions of the other $3\,^3D \to 2\,^3P$ radiative transitions (see Fig. 1). The light intensities $I_1(t)$ and $I_2(t)$ emitted in these two spectral components can be written

$$I_1(t)=KN_1(t)A_{3\,^3D_1\rightarrow 2\,^3P_0},$$
$$I_2(t)=K[N_3(t)A_{3\,^3D_3\text{-}2\,^3P_2}+N_2(t)(A_{3\,^3D_2\rightarrow 2\,^3P_2}+A_{3\,^3D_2\rightarrow 2\,^3P_1})+N_1(t)(A_{3\,^3D_1\rightarrow 2\,^3P_2}+A_{3\,^3D_1\rightarrow 2\,^3P_1})], \quad (1)$$

where K, $N_1(t)$, $N_2(t)$, and $N_3(t)$ are respectively a constant and the population densities of the $3\,^3D_1$, $3\,^3D_2$, and $3\,^3D_3$ sublevels. The $A_{\alpha J\rightarrow\alpha' J'}$ are the transition probabilities of the $\alpha J\rightarrow\alpha' J'$ radiative transitions and are deduced from the individual line strengths.[9] Since we cannot distinguish, from spectroscopic measurements, the population variations on the $3\,^3D_2$ and $3\,^3D_3$ sublevels, in the following they are considered as one state, $3\,^3D_{2,3}$, the population of which is $N_{2,3}(t)=N_2(t)+N_3(t)$. Numerically system (1) becomes

$$I_1(t)=QN_1(t)(0.392),$$
$$I_2(t)=Q[N_{2,3}(t)(0.706)+N_1(t)(0.314)], \quad (2)$$

where Q is a constant.

A population variation is induced on the $3\,^3D_1$ sublevel by selective pumping of the $3\,^3D_1\rightarrow 2\,^3P_0$ transition. Fluorescence is only detected in the $3\,^3D_1\rightarrow 2\,^3P_0$ (resonance fluorescence) and $3\,^3D_{2,3}\rightarrow 2\,^3P_{1,2}$ (induced fluorescence) components. The spectrometer slits are adjusted in order to integrate the light intensity emitted in each spectral component on its profile while keeping a good separation between them (see Fig. 1). Particularly in all experiments, we have checked that stray laser light ($\lambda_L=5875.97$ Å) is not detected when the spectrometer is tuned to the induced-fluorescence wavelength ($\lambda=5875.63$ Å).

We have shown in Ref. 3 that the collisional couplings between the $3\,^3D$, $3\,^3P$, and $3\,^3S$ He I levels are sufficiently weak that in the pressure range under study the $3\,^3D$-level population behaves almost independently. Indeed, in the present experiment no significant transfer is detected in the $3\,^3S$ and $3\,^3P$ states, so that we can neglect the contributions of the back processes,

$$\text{He}(3\,^3P)+\text{He}\rightarrow\text{He}(3\,^3D)+\text{He},$$
$$\text{He}(3\,^3S)+\text{He}\rightarrow\text{He}(3\,^3D)+\text{He}, \quad (3)$$

to the $3\,^3D_{1,2,3}$ sublevel populations.

The "perturbated system" reduces to the $3\,^3D_1$ and $3\,^3D_{2,3}$ states, whose population variations $\Delta N_i(t)$ are described in relaxation regime (laser-free) by the rate equations:

$$\frac{d\Delta N_1(t)}{dt}=-\Delta N_1(t)(A_{3\,^3D_1}+R_{3\,^3D_1}n_{\text{He}}+S_{3\,^3D_1}n_e)+\Delta N_{2,3}(t)(R_{2,3\rightarrow 1}n_{\text{He}}+S_{2,3\rightarrow 1}n_e),$$
$$\frac{d\Delta N_{2,3}(t)}{dt}=\Delta N_1(t)(R_{1\rightarrow 2,3}n_{\text{He}}+S_{1\rightarrow 2,3}n_e)-\Delta N_{2,3}(t)(A_{3\,^3D_{2,3}}+R_{3\,^3D_{2,3}}n_{\text{He}}+S_{3\,^3D_{2,3}}n_e). \quad (4)$$

In Eq. (4), $A_{3\,^3D_1}$ and $A_{3\,^3D_{2,3}}$ are the total radiative transition probabilities of the $3\,^3D_1$ and $3\,^3D_{2,3}$ states; $R_{3\,^3D_1}$ ($S_{3\,^3D_1}$) and $R_{3\,^3D_{2,3}}$ ($S_{3\,^3D_{2,3}}$) are the total quenching rate coefficients for atomic (electronic) collisions. n_{He} and n_e, respectively, represent the atomic and electronic population number

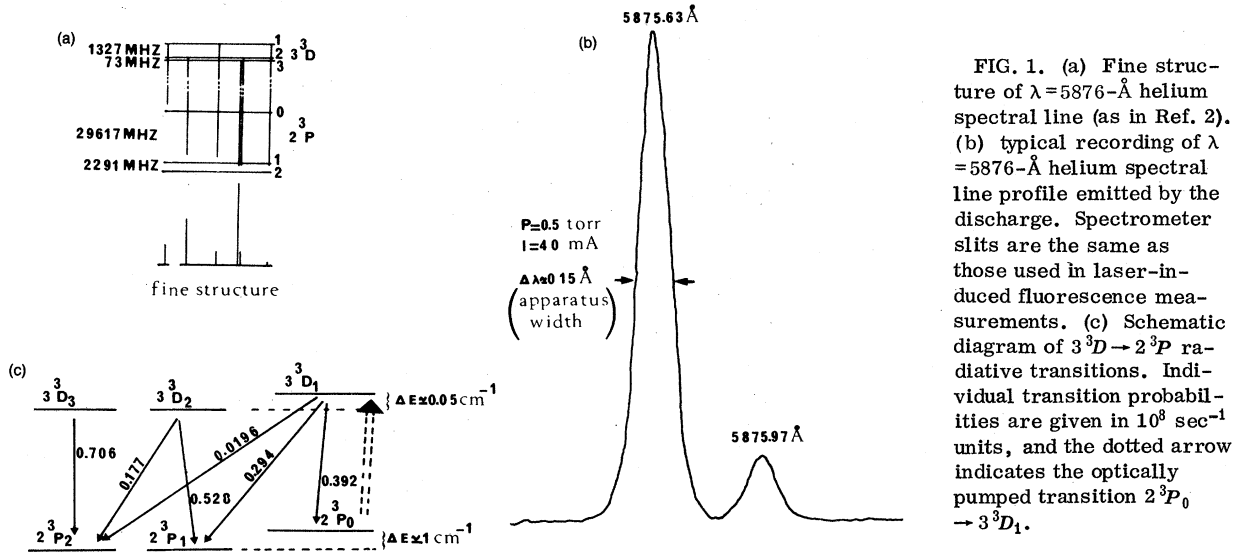

FIG. 1. (a) Fine structure of $\lambda=5876$-Å helium spectral line (as in Ref. 2). (b) typical recording of $\lambda=5876$-Å helium spectral line profile emitted by the discharge. Spectrometer slits are the same as those used in laser-induced fluorescence measurements. (c) Schematic diagram of $3\,^3D\rightarrow 2\,^3P$ radiative transitions. Individual transition probabilities are given in 10^8 sec^{-1} units, and the dotted arrow indicates the optically pumped transition $2\,^3P_0\rightarrow 3\,^3D_1$.

densities. Furthermore, $R_{2,3\to1}$ and $S_{2,3\to1}$ (and, respectively, $R_{1\to2,3}$ and $S_{1\to2,3}$) are the rate coefficients for the reactions:

$$\mathrm{He}(3\,^3D_{2,3})+\mathrm{He}\underset{R_{1\to2,3}}{\overset{R_{2,3\to1}}{\rightleftharpoons}}\mathrm{He}(3\,^3D_1)+\mathrm{He}, \tag{5}$$

$$\mathrm{He}(3\,^3D_{2,3})+e\underset{S_{1\to2,3}}{\overset{S_{2,3\to1}}{\rightleftharpoons}}\mathrm{He}(3\,^3D_1)+e. \tag{6}$$

Equations (4) may be written in vector form:

$$\frac{d\Delta\vec{N}}{dt}=A\Delta\vec{N}, \tag{7}$$

where A is a square matrix of order 2.

The quantities $\Delta N_1(t)$ and $\Delta N_{2,3}(t)$ are deduced from measurements of the variation of resonance- and induced-fluorescence intensities $\Delta I_2(t)$ and $\Delta I_1(t)$ by relations (2).

IV. RESULTS

For various experimental situations (P_{He}, i), the relaxation curves are analyzed using the identification method extensively described in a previous paper.[3] Let us just recall that the coefficients a_{ij} of matrix A intervening in Eq. (7) are determined so as to minimize the difference between experimental curves and solutions of Eq. (7). An example of identification is shown in Fig. 2 for two pressure values.

The coefficients of matrix A do not depend on discharge current intensity i, so that the electronic contributions in Eq. (4) are negligible. However, as expected, they depend linearly on the helium pressure:

$$a_{ij}=\alpha_{ij}+\beta_{ij}P_{\mathrm{He}}. \tag{8}$$

These coefficients are plotted in Fig. 3 as functions of the helium pressure. Confidence intervals are obtained through numerical data analysis by varying the experimental points in their error bars. For radiative coefficients we obtain

$$\begin{aligned}\alpha_{11}&=A_{3\,^3D_1}=(7.3\pm0.4)\times10^7\ \mathrm{sec}^{-1},\\ \alpha_{22}&=A_{3\,^3D_{2,3}}=(6.4\pm0.5)\times10^7\ \mathrm{sec}^{-1}\end{aligned} \tag{9}$$

values which are in good agreement with previous measurements[3] $A_{3\,^3D}=(6.56\pm0.07)\times10^{-7}$ sec^{-1} and the accepted result[10] $(7.06\pm0.2)\times10^{-7}$ sec^{-1}. For collisional quenching coefficients we obtain

$$\begin{aligned}\beta_{11}&=(9.4\pm1)\times10^7\ \mathrm{sec}^{-1}\mathrm{torr}^{-1},\\ \beta_{22}&=(3\pm1)\times10^7\ \mathrm{sec}^{-1}\mathrm{torr}^{-1},\end{aligned} \tag{10}$$

and for collisional excitation transfer coefficients we obtain

$$\begin{aligned}\beta_{12}&=(9\pm3)\times10^7\ \mathrm{sec}^{-1}\mathrm{torr}^{-1},\\ \beta_{21}&=(2.3\pm0.3)\times10^7\ \mathrm{sec}^{-1}\mathrm{torr}^{-1}.\end{aligned} \tag{11}$$

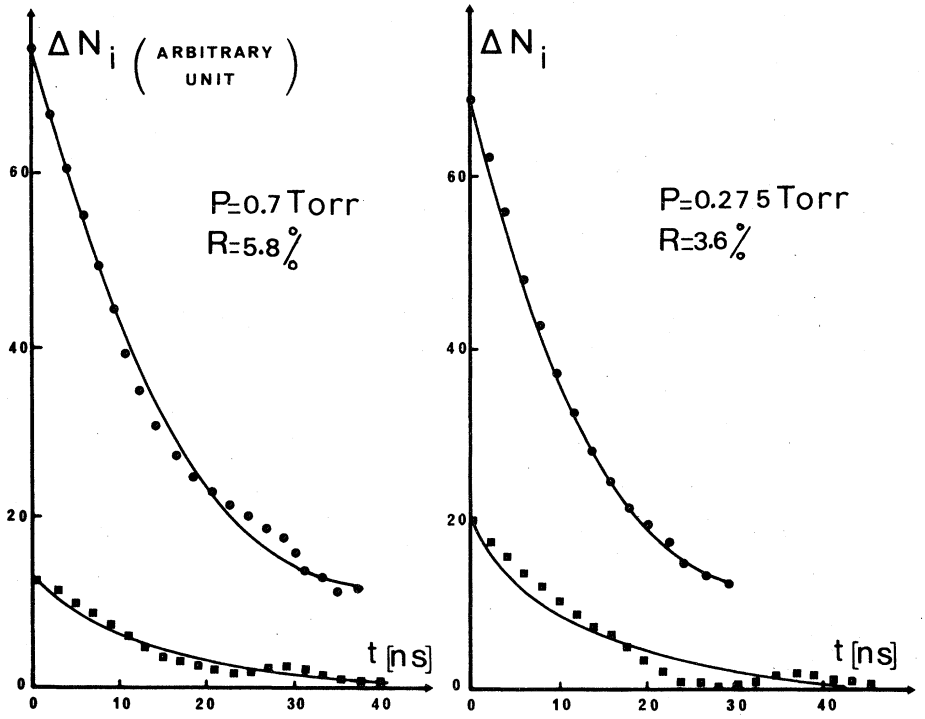

FIG. 2. Comparison, for two helium-pressure values, of results given by the identification method (continuous curves) and the experimental relaxation curves: ●, $3\,^3D_{2,3}$ population variation relaxation; ■, $3\,^3D_1$ population variation relaxation. R is the residual identification error.

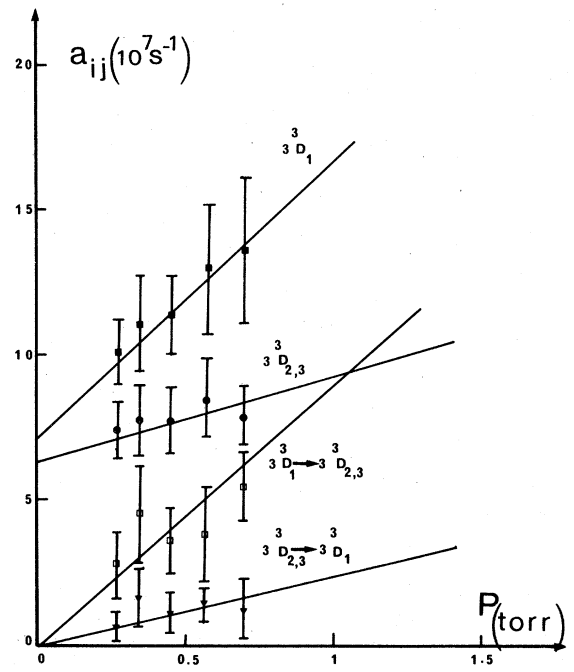

FIG. 3. Coefficients a_{ij} of matrix A [see Eq. (7)] as functions of the helium pressure: total destruction coefficient of the $3\,^3D_1$ state a_{11} (■); total destruction coefficient of the $3\,^3D_{2,3}$ state a_{22} (●); excitation transfer coefficient $3\,^3D_1 \rightarrow 3\,^3D_{2,3} a_{12}$ (□); excitation transfer coefficient $3\,^3D_{2,3} \rightarrow 3\,^3D_1 a_{21}$ (▼).

The velocity-averaged cross sections deduced from the β_{ij} are summarized in Table I. We observe that $\bar{\sigma}_{3\,^3D_1} \simeq \bar{\sigma}_{1\rightarrow 2,3}$ and $\bar{\sigma}_{3\,^3D_{2,3}} \simeq \bar{\sigma}_{2,3\rightarrow 1}$.[11] This indicates that for $P_{He} < 1$ torr the quenching processes of each considered state are mainly due to fine-structure-changing collisions. For higher-pressure values ($P_{He} > 2$ torr), these efficient processes tend to equilibrate the populations within the fine structure with characteristic times much shorter than the time resolution of our experiment. Under these conditions, we observe only the quenching processes of the $3\,^3D$ level as a whole outside the fine structure, mainly $3\,^3D \rightarrow 3\,^3P$ excitation transfer and associative ionization, as reported in Ref. 3.

TABLE I. Thermally averaged quenching cross sections $\bar{\sigma}_{3\,^3D_1}$ and $\bar{\sigma}_{3\,^3D_{2,3}}$ of the $3\,^3D_1$ and $3\,^3D_{2,3}$ states, and thermally averaged excitation transfer cross sections [reaction (5)] $\bar{\sigma}_{2,3\rightarrow 1}$ and $\bar{\sigma}_{1\rightarrow 2,3}$.

	$\bar{\sigma}$ (Å^2)
$\bar{\sigma}_{3\,^3D_1}$	175 ± 15
$\bar{\sigma}_{3\,^3D_{2,3}}$	60 ± 20
$\bar{\sigma}_{2,3\rightarrow 1}$	42 ± 5
$\bar{\sigma}_{1\rightarrow 2,3}$	180 ± 60

V. CONCLUSION

Despite the quasiresonant character of the studied excitation transfer (energy gap ~0.05 cm^{-1}), the measured cross sections $\bar{\sigma} < 200$ Å^2 imply that for low-pressure values ($P_{He} \lesssim 0.1$ torr) a nonstatistical population redistribution can be obtained for the $3\,^3D_1$ and $3\,^3D_{2,3}$ helium states. Measurements of the line-component intensity ratio performed in one continuous operation as a function of the helium pressure confirm this result.

The experimental ratio $\bar{\sigma}_{2,3\rightarrow 1}/\bar{\sigma}_{1\rightarrow 2,3} = 0.23 \pm 0.1$ agrees well with the theoretical value of 0.25 given by the microreversibility principle. Moreover, the obtained cross sections are of the same order of magnitude as that proposed by Cahuzac *et al.*[2] for the $2\,^3P_1 \rightarrow 2\,^3P_2$ excitation transfer ($\bar{\sigma}_{2\,^3P_1 \rightarrow 2\,^3P_2} \simeq 70$ Å) in a helium glow discharge.

As proposed for the cases of alkaline-rare-gas and Na($3\,^2P$)-Hg fine-structure-changing collisions,[12] the observed $3\,^3D_1 \rightarrow 3\,^3D_{2,3}$ excitation transfer in helium suggests a long-range potential curve crossing of the two states.

[1] L. Krauze, Adv. Chem. Phys. 28, 267 (1975).
[2] P. Cahuzac and R. Damaschini, Opt. Commun. 20, 111 (1977).
[3] B. Dubreuil and A. Catherinot, Phys. Rev. A 21, 188 (1980).
[4] A. Catherinot, B. Dubreuil, and M. Gand, Phys. Rev. A 18, 1097 (1978).
[5] A. Catherinot, P. Placidet, and B. Dubreuil, J. Phys. B 11, 3775 (1978).
[6] A. Catherinot and A. Sy, Phys. Rev. A 20, 1511 (1979).
[7] R. D. Kaul, J. Opt. Soc. Am. 58, 429 (1968).
[8] A. Kponou, V. W. Hughes, C. E. Johnson, S. A. Lewis, and F. M. J. Pichanick, Phys. Rev. Lett. 26, 1613 (1974).
[9] B. W. Shore and D. H. Menzel, *Principles of Atomic Spectra* (Wiley, New York, 1968).
[10] W. L. Wiese, H. W. Smith, and B. M. Glennon, Natl. Stand. Ref. Data Ser. Natl. Bur. Stand. 1, 4 (1966).
[11] The slight difference between the $\bar{\sigma} 3\,^3D_{2,3}$ and $\bar{\sigma}_{2,3\rightarrow 1}$ experimental mean values may be partly attributed to the associative ionization process $He(3\,^3D_{2,3}) + He(1\,^1S) \rightarrow He_2^+ + e^-$.
[12] R. Düren, Chem. Phys. Lett. 39, 481 (1976).